Optimizing the Receiving Properties of Electrically Small HF Antennas

Steven R. Best

MITRE Corporation
Bedford, MA 01730 USA
E-mail: sbest@mitre.org

Abstract

Because of the large operating wavelength, receiving antennas in the high-frequency (HF: 3 MHz to 30 MHz) operating band are often electrically small. It is well known that electrically small antennas generally exhibit low radiation efficiency, and are difficult to match over wide bandwidths. In the HF band, external background noise is high, and receiving systems are ideally designed to ensure that the system remains externally noise limited. In this paper, we discuss the properties of the general, electrically small, receiving antenna. We present formulas that can be used to determine, characterize, and compare the performance of the general, electrically small, receiving antenna. We demonstrate that optimization of the small HF antenna's receiving-performance parameters, such as its receiving sensitivity and noise figure, are directly a function of optimizing the antenna's impedance match and radiation efficiency, independently of whether a dipole, monopole, or loop-like design is utilized. We demonstrate that impedance matching for the receiving antenna is often a secondary consideration. We illustrate differences in an antenna's matching-network transfer function for the receiving mode versus the transmitting mode. We present formulas and design guidelines for optimizing the receiving system's noise figure and signal-to-noise ratio performance. Finally, we present design examples for an electrically small dipole, loop, and multi-turn loop.

1. Introduction

The HF band has been in use almost since the beginning of radio communication. For many decades, HF has been used in long-range military communications, amateur radio, and long-range over-the-horizon radar (OTHR) [1-3]. More recently, HF is being used in applications such as radio-frequency identification (RFID), and higher-data-rate communications, such as HF multiple-input multiple-output (MIMO) [4, 5]. While these applications use both transmitting and receiving antennas, this paper presents a discussion on optimizing the performance properties of the general, electrically small, HF receiving antenna.

We begin with a discussion of the properties of the general receiving antenna from the equivalent-circuit perspective. Formulas are presented for the open-circuit voltage at the receiving antenna's feed-point terminal. These formulas are subsequently used to derive expressions for the receiving sensitivity of the general antenna.

Section 2 of the paper presents a background discussion on the basic properties of the electrically small dipole and multi-turn loop, which are commonly used as receiving antennas in the HF band. Design formulas for characterizing the small antenna's radiation resistance, loss resistance, and therefore the radiation efficiency are presented. In Section 3 of the paper, we derive several expressions for the receiving sensitivity of the small multi-turn loop, as well as for the general receiving antenna. We show that the receiving sensitivity of the electrically small antenna can be expressed in terms of any of the electromagnetic (EM) wave's constituent parameters: power density, electric field, magnetic field, electric-flux density, or magnetic-flux density, independently of whether the antenna is a dipole or loop-like design.

In Section 4 of the paper, we discuss impedance-matching considerations for the receiving antenna. We illustrate that impedance matching is a secondary consideration, as a matching network designed from the transmitting perspective may not improve the antenna's performance for receiving. In Section 5 of the paper, we discuss external noise, noise figure, and signal-to-noise ratio (*SNR*) for a typical receiving system. We present formulas and design guidelines that aid in optimizing system performance from a signal-to-noise ratio perspective. Finally, we present design examples for electrically small dipole and loop antennas, comparing their performance in a typical receiving system.

We note that in the derivations and formulas that follow in this paper, we have assumed that the values of

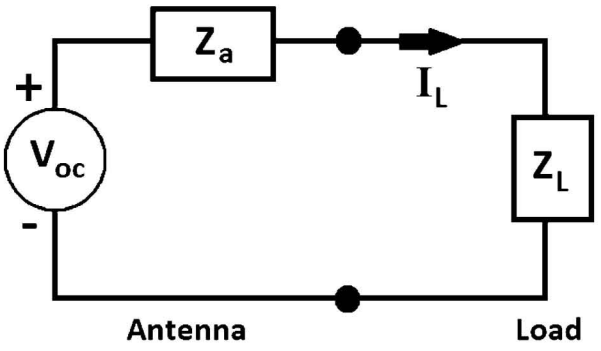

Figure 1. A depiction of the equivalent circuit of the general receiving antenna.

voltage (V), current (I) and field strength (E and H) are peak values, rather than rms values. As a result, power and power-density formulas are written in the form of $1/2|I|^2 R$ and $1/2|E|^2/120\pi$, rather than $|I|^2 R$ and $|E|^2/120\pi$, respectively.

2. The General Receiving Antenna

In recent years, there have been many papers in the literature that focused on specific designs of electrically small antennas in general, as well as specifically on HF antennas (e.g., [6-9]). HF-antenna papers have generally presented the performance properties of a specific antenna design, but they have often not considered the optimization of the HF antenna's performance within its operating environment, nor do they usually consider how the antenna properties affect the performance of the overall HF system. It is well understood that HF antennas operate in complex and noisy EM environments, and that the HF antenna's performance is established by the antenna's design, as well as by the interactions with the platform on which it is installed (vehicle, ship, aircraft, etc.), which often becomes the dominant radiator. Furthermore, to accurately characterize the HF antenna's performance, the details of the RF grounding system and antenna interactions with the Earth ground must also be considered. These issues are often beyond the scope of an antenna-design paper, because they are difficult to characterize, and they are dependent on the specific details of the antenna's installation.

When optimizing the performance properties of transmitting antennas – particularly those that are electrically small – antenna engineers primarily focus on impedance matching, matched impedance bandwidth, and radiation efficiency. With electrically small antennas, the directivity pattern and polarization properties are oftentimes secondary considerations. With the general receiving antenna, the impedance match and radiation efficiency also ultimately determine how well the antenna's performance is optimized. However, there are some subtleties to consider that are unique to the receiving antenna. These include the fact that impedance-matching considerations are different for the receiving antenna, and that the receiving system's performance is ultimately established by the signal-to-noise ratio at the detection point in the receiver.

In this section of the paper, we briefly review the electromagnetic and circuit perspectives of the receiving properties of the general antenna. We discuss the most general equivalent circuit of the receiving antenna and the determination of received power as functions of the incident EM wave properties: power density, P_d ($\mathrm{W/m^2}$); electric-field strength, E ($\mathrm{V/m}$); and magnetic-field strength, H ($\mathrm{A/m}$).

The power received by the general antenna, P_r, is given by [10, 11]

$$P_r = P_d \tau \eta_r \frac{\lambda^2 D}{4\pi}, \qquad (1)$$

where λ is the operating wavelength, η_r is the antenna's radiation efficiency, D is the antenna's directivity in the direction of the incident EM wave, and τ is the receiving antenna's mismatch loss. τ is given by

$$\tau = \frac{4R_a R_L}{|Z_a + Z_L|^2}, \qquad (2)$$

where Z_a is the antenna's impedance, Z_L is the load impedance connected at the antenna's feed point, R_a is the antenna's resistance (including both the radiation, R_r and loss, R_l, resistances), and R_L is the load resistance.

To determine received power using circuit theory, we begin with the Thevenin equivalent circuit for the general receiving antenna shown in Figure 1. For the purposes of determining received power, this equivalent circuit is valid for all antennas. The important consideration is the correct determination of the Thevenin circuit's open-circuit voltage.

For an antenna operating in frequency regions near its series resonance (resonance), where the radiation and loss resistances are in series, the open-circuit voltage is given by [11]

$$|V_{oc}| = \frac{|E|\lambda}{\pi}\sqrt{\frac{R_r D}{120}} = \frac{|E|\lambda}{\pi}\sqrt{\frac{\eta_r R_a D}{120}}. \qquad (3)$$

For an antenna operating in frequency regions near its parallel resonance (anti-resonance), where the radiation and loss resistances are in parallel, the open-circuit voltage is given by [11]

$$|V_{oc}| = \frac{|E|\lambda}{\pi}\sqrt{\frac{{\eta_r}^2 R_r D}{120}} = \frac{|E|\lambda}{\pi}\sqrt{\frac{\eta_r R_a D}{120}}. \qquad (4)$$

When expressed in terms of the antenna's total feedpoint resistance rather than the radiation resistance, both formulas are identical. For electrically small antennas, where expressions for the antenna's radiation resistance can be derived and where the directivity approaches a value of approximately 1.5, Equations (3) and (4) can be further simplified and written in terms of the antenna's physical dimensions. Additionally, we note that while Equations (3) and (4) are written in terms of the incident electric-field strength, they can also be written in terms of the incident power density, magnetic-field strength, electric-flux density, or magnetic-flux density, using the well-known relationships among these quantities. This will be discussed in greater detail in subsequent sections.

From Figure 1, the antenna's received power can be found from

$$P_r = \frac{1}{2}|I_L|^2 R_L, \qquad (5)$$

where I_L is given by

$$I_L = \frac{V_{oc}}{Z_a + Z_L}. \qquad (6)$$

We note that Equations (5) and (1) yield identical results.

3. The Electrically Small Dipole and Loop

The most fundamental antenna elements that can be used as HF receiving antennas are the electrically small straight-wire dipole and circular loop, shown in Figure 2. The straight-wire dipole has an overall conductor length l, and the circular loop has a conductor length (circumference) C, and an area A. We note that the monopole antenna is commonly used as an HF receiving antenna, as well. We do not explicitly discuss the performance of the monopole, since its behavior is similar to that of the dipole.

The dipole and loop are electrically small for values of ka less than 0.5 [12], where k is the free-space wavenumber, $2\pi/\lambda$, and a is the radius of a sphere circumscribing the maximum dimension of the antenna. As the value of ka decreases, the radiation resistances of the dipole and the loop approach zero, and are given by [10]

$$R_{rd} \approx 20\pi^2\left(\frac{l}{\lambda}\right)^2, \qquad (7)$$

and

$$R_{rl} \approx 320\pi^4 N^2\left(\frac{A}{\lambda^2}\right)^2, \qquad (8)$$

respectively. N is the number of turns in the loop. We note that Equation (8) is valid for electrically small loops of any geometry.

A comparison of Equations (7) and (8) reveals several important facts about the relative performance of electrically small dipoles and loops. The dipole's radiation resistance diminishes as $1/\lambda^2$, whereas the loop's radiation resistance diminishes as $1/\lambda^4$. For this reason, a loop antenna having the same conductor length as a dipole will be substantially less efficient than the dipole. However, that does not preclude the use of the loop as an effective receiving antenna, since, as seen in Equation (8), the radiation resistance, and therefore its efficiency, can be increased by increasing the number of turns. When adding turns, the loop's loss resistance increases by N, whereas its radiation resistance increases by N^2. The radiation resistance and efficiency of the small loop can be further increased by winding the loop's turns on a ferrite core. When the loop's turns are wound on a ferrite core, the loop's radiation resistance becomes [10]

$$R_{rl} \approx 320\pi^4 {\mu_{cr}}^2 N^2\left(\frac{A}{\lambda^2}\right)^2. \qquad (9)$$

μ_{cr} is the effective relative permeability of the core, given by

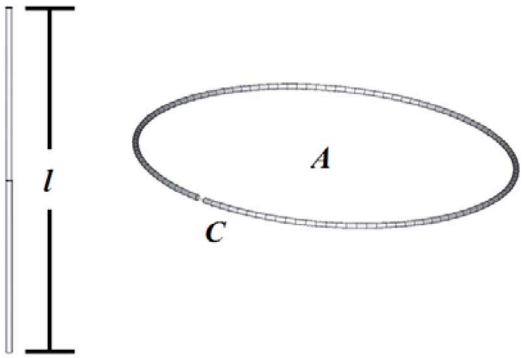

Straight Wire Dipole **Circular Loop**

Figure 2. Depictions of the straight-wire dipole having an overall length, l, and the circular loop having a conductor length, C, and area, A.

$$\mu_{cr} = \frac{\mu_{fr}}{1 + D_m\left(\mu_{fr} - 1\right)}, \qquad (10)$$

where μ_{fr} is the relative permeability of the unbounded ferrite, and D_m is the demagnetization factor, which is related to the core's geometry. The value of μ_{fr} is generally taken to be the relative permeability of the ferrite material provided by the manufacturer. The value of D_m varies with the core's geometry. For a cylindrical core with length, $2l$, greater than its radius, a, D_m can be approximated by the value of D_m of an ellipsoid, given by [10]

$$D_m = \left(\frac{a}{l}\right)^2\left[\ln\left(\frac{2l}{a}\right) - 1\right], \quad l \gg a. \qquad (11)$$

Another advantage of the electrically small receiving loop is that the magnitude of its reactance is generally much smaller than that of the dipole. The electrically small dipole typically has a high value of capacitive reactance, making it relatively difficult to tune, because this generally would require a large series variable inductor. The loop antenna typically has a low inductive reactance, which makes tuning relatively easy with a variable series capacitor. Oftentimes, small multi-turn, ferrite-core loops are used as simple receiving antennas for the reasons discussed above. Their performance properties will be discussed in more detail in a subsequent section.

The radiation resistances of the electrically small loop and dipole often approach zero, and are therefore a small component of their total feed-point resistance. To determine the antenna's total resistance and radiation efficiency, it is necessary to determine its loss resistance. This can often be estimated by the conductor's length and its dc resistance per unit length.

The loss resistance of an electrically small dipole having a conductor diameter, d, is approximated by [13, 14]

$$R_{le} \approx \frac{l\rho}{3\pi d\delta} \approx \frac{l}{3\pi d}\sqrt{\frac{kc\mu_0\rho}{2}}, \qquad (12)$$

where ρ is the resistivity of the wire, and μ_0 is the permeability of free space. In Equation (12), the skin depth, δ, in the conductor is assumed to be somewhat less than $d/2$. For δ somewhat greater than $d/2$, the loss resistance of the electrically small dipole can be approximated as

$$R_{le} \approx \frac{2l\rho}{\pi d^2}. \qquad (13)$$

To obtain the approximation of loss resistance in Equation (12), we assume that the current has a triangular dependence over the length of the conductor, and that the current density decays exponentially from its value at the surface of the conductor.

The loss resistance of the electrically small, multi-turn circular loop of radius r can be approximated as

$$R_{lm} \approx \frac{2Nr\rho}{d\delta} \approx \frac{2Nr}{d}\sqrt{\frac{kc\mu_0\rho}{2}}. \qquad (14)$$

For an arbitrarily shaped loop of area A, Equation (14) can be written as

$$R_{lm} \approx \frac{2N}{d}\sqrt{\frac{kc\mu_0\rho A}{2\pi}}. \qquad (15)$$

For δ somewhat greater than $d/2$, the loss resistance of the small circular loop can be approximated as

$$R_{lm} \approx \frac{8N\rho}{d^2}\sqrt{\frac{A}{\pi}}. \qquad (16)$$

Here, we assume that the current does not vary around the loop, and that the current density decays exponentially from its value at the surface of the wire.

The final points we make in this section are with regard to the general EM receiving behavior of the electrically small dipole and loop. The electrically small dipole is often referred to as an electric-dipole, because it exhibits the fundamental-mode radiation pattern of a simple dipole from low frequencies ($ka \ll 0.5$) through its first natural resonance. The loop antenna is often referred to as a magnetic-dipole, because it is assumed to exhibit the fundamental-mode radiation pattern of a magnetic-dipole. At very small values of ka, ($ka \ll 0.5$), the loop will exhibit the radiation pattern of a magnetic-dipole. As ka starts to approach values above 0.1, the null in the direction of the loop's axis degrades, and the magnetic-dipole pattern will no longer hold.

Another and perhaps more significant point relates to the responses of the dipole and loop to incident electromagnetic fields. The dipole is often presumed to sense or detect the electric field, and the loop is often presumed to sense or detect the magnetic field. In the case of an incident far-field EM wave, the dipole and loop both respond to the electric and magnetic fields. Performance properties, such as received power, open-circuit voltage,

receiving sensitivity, etc., can be written in terms of the electric field, magnetic field, electric-flux density, and magnetic-flux density for both the dipole and loop. This will be illustrated in subsequent sections.

4. Receiving Sensitivity

One of the common parameters used to characterize the effectiveness of a receiving antenna is its receiving sensitivity. This is defined as the minimum strength of the incident EM wave that results in a received power equal to the thermal noise in 1 Hz of bandwidth, $k_b T_0$, where k_b is Boltzmann's constant, and T_0 is typically taken as the Nyquist temperature, 290K [15].

For the general receiving antenna, the sensitivity is oftentimes derived using the circuit diagram of Figure 1, the received power of Equation (5), and the appropriate choice of field quantity. We note that sensitivity can be defined in terms of the incident power density, electric-field, magnetic-field, electric-flux density, or magnetic-flux density for both the electrically small dipole and loop.

A common approach with the multi-turn, electrically small, air-core loop is to begin with the following expression for the open-circuit voltage [10]:

$$V_{oc} = j2\pi fNAB\,, \tag{17}$$

where f is the operating frequency and B is the incident magnetic-flux density (Tesla). In Equation (17), we assume that the magnetic-field lines are normal to the loop axis (the incident EM wave is co-polarized with the loop).

Assuming that the multi-turn loop is conjugate matched to the receiving system ($X_L = -X_a$ and $R_L = R_a$), the power delivered to the receiving system is given by $1/2|I_L|^2 R_a$, where $|I_L| = |V_{OC}|/(2R_a)$. Setting the received power equal to $k_b T_0$ and substituting Equation (17) for V_{OC}, the receiving sensitivity, S (in units of $\mathrm{T}/\mathrm{Hz}^{1/2}$) can be expressed as

$$S_B = \frac{\sqrt{2R_a k_b T_0}}{\pi fNA}\,, \tag{18}$$

where R_a, the antenna's resistance, is the sum of the radiation and loss resistances. For many electrically small loop antennas, R_a can simply be approximated by the loss resistance. We note that for the ferrite-core loop, the open-circuit voltage becomes $V_{oc} = j2\pi f \mu_{cr} NAB$, and μ_{cr} is added to the denominator of Equation (18) to determine its sensitivity. The sensitivity of the ferrite-core loop improves in direct proportion to the effective core permeability, μ_{cr}.

To express the sensitivity of the air-core loop in terms of the EM wave's other field quantities, we simply express the open-circuit voltage in terms of the appropriate field quantity. The commonly used expression for the open-circuit voltage of the electrically small, multi-turn, air-core loop is given in Equation (17) as a function of magnetic-flux density. Given the constituent relationships $B = \mu H$, $|E/H| = 120\pi$, and $P_d = 1/2|E|^2/120\pi$, we can write the open-circuit voltage, and therefore the receiving sensitivity, in terms of E, H, and P_d. Substituting Equation (8) into Equation (3) and assuming an electrically small antenna directivity of 1.5, we can express the open-circuit voltage of the multi-turn, air-core loop in terms of the electric field and magnetic field as

$$|V_{oc}| = kNAE \tag{19}$$

and

$$|V_{oc}| = k120\pi NAH\,, \tag{20}$$

respectively. We note that Equations (19) and (20) will yield the same result as Equation (17) for the magnitude of the open-circuit voltage.

Following the method used to arrive at Equation (18), the sensitivity of the multi-turn, air-core loop can be expressed (in units of $(\mathrm{V/m})/\mathrm{Hz}^{1/2}$) as

$$S_E = \frac{\sqrt{8R_a k_b T_0}}{kNA}\,. \tag{21}$$

The receiving sensitivities as expressed in Equations (18) and (21) provide some insight into how the physical properties of the multi-turn, air-core loop improves with an increase in the number of turns and the loop area. Increasing the number of turns and increasing the loop area improves sensitivity. We note that the results of Equations (18) and (21) differ by the relationships of the constituent parameters of the incident EM wave.

While these expressions are valuable in understanding the design of the small multi-turn loop, they do not provide insight into how the sensitivity of the electrically small loop compares to other electrically small antennas, such as a dipole or a monopole. Furthermore, these expressions were derived assuming the receiving system was conjugate matched to the loop's impedance. Knowing that mismatch and ohmic loss degrade a receiving antenna's sensitivity, we desire a formula for receiving sensitivity expressed in terms of mismatch and ohmic loss that is valid for the general, electrically small receiving antenna.

We start by deriving the sensitivity, S_E, using the form of Equation (3) containing the total feed-point

resistance, R_a. This yields a received sensitivity (in units of $(\mathrm{V/m})/\mathrm{Hz}^{1/2}$), valid for the general receiving antenna, expressed as

$$S_E = k\sqrt{\frac{240k_bT_0}{\eta_r D}}. \qquad (22)$$

While Equation (22) is valid for the general, electrically small receiving antenna, we note that Equation (21) will only be valid for the multi-turn loop provided that $D = 1.5$, and Equation (8) is an accurate approximation of the radiation resistance of the loop. For the general electrically small antenna, where $D = 1.5$, Equation (22) becomes

$$S_E = k\sqrt{\frac{160k_bT_0}{\eta_r}}. \qquad (23)$$

Given the relationship among received power and mismatch and ohmic loss, Equation (23) can be modified to include mismatch loss as follows:

$$S_E = k\sqrt{\frac{160k_bT_0}{\tau\eta_r}}. \qquad (24)$$

A similar derivation holds for expressing the receiving sensitivity of the general electrically small antenna in units of $(\mathrm{A/m})/\mathrm{Hz}^{1/2}$. In this case, the sensitivity is expressed as

$$S_H = k\sqrt{\frac{k_bT_0}{90\pi^2\tau\eta_r}}. \qquad (25)$$

An alternate approach to deriving an expression for receiving sensitivity for any antenna is to begin with Equation (1), which is an expression of received power in terms of mismatch loss, radiation efficiency, and directivity. Setting the received power to k_bT_0, the general antennas' receiving sensitivity (in units of $(\mathrm{W/m^2})/\mathrm{Hz}^{1/2}$) is expressed as

$$S_P = \frac{4\pi k_bT_0}{\lambda^2\tau\eta_r D}. \qquad (26)$$

There are two significant points regarding the general receiving antenna discussed in this section. The first is the fact that all receiving antennas respond to both the incident electric and magnetic fields. The dipole does not respond only to the electric field and the loop does not respond only to the magnetic field. As a result, performance characteristics, such as received power, open-circuit voltage, and receiving sensitivity, can be expressed in terms of any of the EM wave's properties. Finally, the most important point is the recognition that the absolute and relative performance of any electrically small antenna are simply determined by its mismatch loss and radiation efficiency. Optimizing the receiving performance of any antenna is a function of optimizing the antenna's impedance match and radiation efficiency. This will be illustrated and discussed in more detail in the following sections.

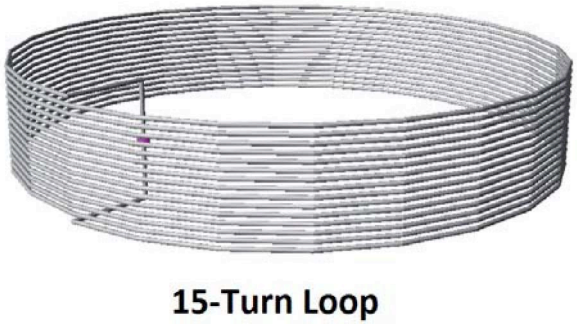

Figure 3. A depiction of the 15-turn air-core loop modeled in *NEC*. The loop had a diameter of 5.08 cm and an overall length of 1 cm.

5. The Multi-Turn Air-core Loop

To validate the discussion and results of the previous sections, we consider the multi-turn air-core loop. Specifically, we consider the electrically small, 15-turn loop shown in Figure 3. The loop had a diameter of 5.08 cm (2 in), an overall length of 1 cm (2.54 cm), and was wound using a copper conductor having a diameter of 0.5 mm (0.02 in). The performance of this antennas was modeled

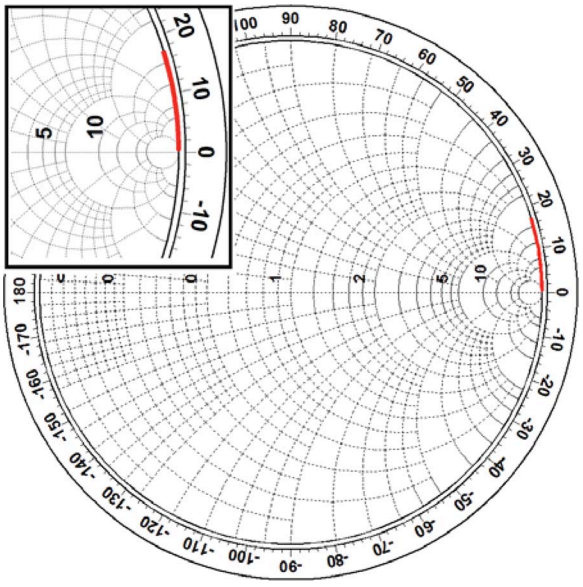

Figure 4. The feed-point impedance of the 15-turn loop antenna. The frequency range was 3 MHz to 30 MHz.

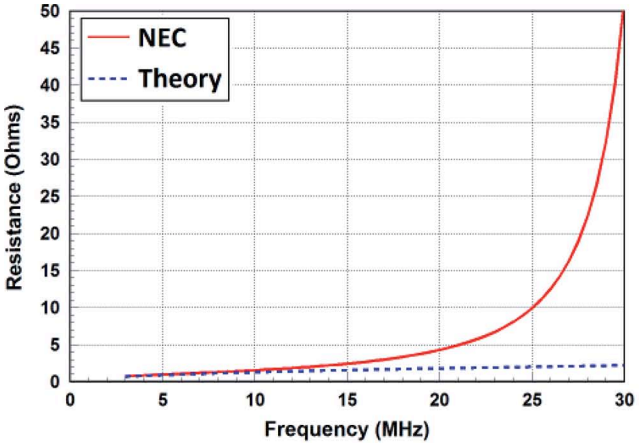

Figure 5. The feed-point resistance of the 15-turn loop antenna.

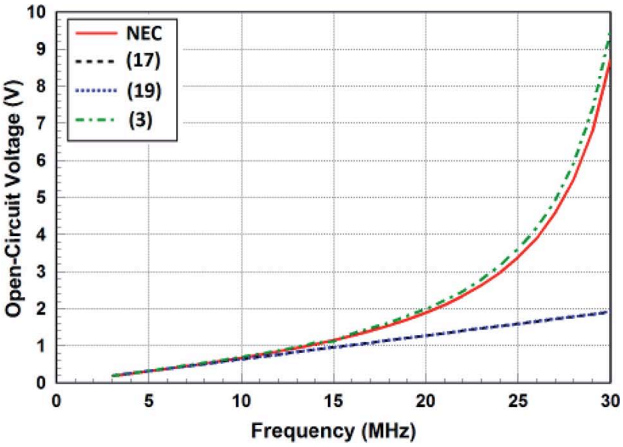

Figure 6. The open-circuit voltage at the feed point of the 15-turn loop antenna.

using the *Numerical Electromagnetics Code* (*NEC*) [16], and the results were compared to the theory presented in the previous sections.

The modeled impedance of the air-core loop is presented in Figure 4. As expected, the total resistance (radiation plus loss) was small, and the reactance varied with frequency as a function of the loop's inductance. The frequency range was 3 MHz to 30 MHz. One of the significant points to note from the Smith chart was the fact that with the 15-turn loop, the upper operating frequency closely approached the loop's first natural resonance. This was an anti-resonance, where the resistance was very large and the radiation and loss resistances were in parallel, rather than being in series. The change in inductance with increasing turns within a loop antenna, which causes the antenna to approach anti-resonance, is even more enhanced when the loop is wound on a ferrite core. For the multi-turn loop, operating near the anti-resonant frequency has a significant impact on the validity of the electrically small approximations for radiation resistance, loss resistance, open-circuit voltage, and sensitivity. These approximations become invalid with an electrically small loop operating near anti-resonance.

The simulated and theoretical resistances and open-circuit voltages are presented in Figures 5 and 6, respectively. The theoretical resistance was calculated from the sum of the radiation-loss resistances using Equations (8) and (15). At low frequencies, where the loop was electrically small, and well away from anti-resonance, theory and simulation were in excellent agreement. We note that at these frequencies, the conductor-loss resistance dominated. Near the anti-resonant frequency, the theoretical approximations were invalid even though the loop was electrically small.

In Figure 6, we saw similar results for the theoretical open-circuit voltage when the antenna was operated near anti-resonance. While Equation (17) was a commonly used expression for the open-circuit voltage of the multi-turn loop, it was not valid in frequency regions where the radiation resistance of the loop could no longer be approximated by Equations (8) or (9). This can be a significant issue with ferrite-core loops, which have a greater tendency to approach anti-resonance than the air-core loop. The invalidity of Equations (8), (9) and (17) also renders the associated, derived calculations for sensitivity invalid.

We note that Equation (3) provided an excellent approximation of the multi-turn, air-core loop's open-circuit voltage, since it is valid for all receiving antennas provided the antenna's performance properties are well known or characterized. Additionally, sensitivity calculations using Equation (26) remain valid for all receiving antennas. The discrepancy in Figure 6 between Equation (3) and *NEC* at the higher frequencies was a result of degradation in the loop's polarization purity, and the fact that the directivity may have deviated from the assumed value of 1.5.

6. Receiving Impedance Matching

When designing HF transmitting antennas, the exercise of impedance matching is critically important. The antenna's voltage standing-wave ratio (*VSWR*) must be minimized to ensure that the HF transmitter is operating at optimal efficiency, and delivering maximum output power to the transmitting system. An increase in *VSWR* will generally cause the transmitter to reduce its output power, or shut off, so as to protect the internal circuits. HF transmitters generally do not operate well into *VSWRs* much greater than 3:1 or 4:1. When utilizing electrically small antennas, some form of impedance-matching network is generally required to ensure that the *VSWR* requirements are satisfied.

When operating over large frequency bandwidths, the minimization of *VSWR* is oftentimes traded against losses within the matching network or within the antenna's structure (e.g., resistively loading the antenna). The matching-network transfer function (S_{21}) is the product or sum of the mismatch loss and the ohmic losses within

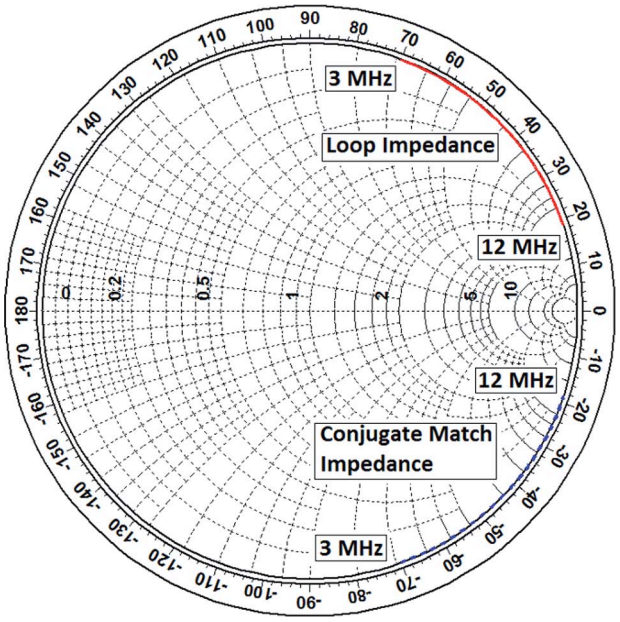

Figure 7. The feed-point impedance of a 1 m diameter circular loop and its conjugate impedance, from 3 MHz to 12 MHz.

the matching-network components. Given a low matched *VSWR*, the frequency response of the S_{21} transfer function is dominated by the network losses. We note that it is theoretically impossible to efficiently impedance match an electrically small antenna over the entire HF band.

For the receiving antenna, the decision to implement an impedance match may be different. Oftentimes, engineers assume that the antenna's *VSWR* equally attenuates signal and external noise, so it does not degrade the receiving system's signal-to-noise ratio. This is true provided the system remains externally noise limited, but this is not always the case. The next section will discuss external noise, *SNR*, and antenna noise figure in more detail. For the remainder of this section, we will defer issues related to the receiving system's *SNR* performance.

We considered the example of a 1-m (39.37 in) diameter circular loop having a conductor diameter equal to 2.63 mm (0.104 in). The feed-point impedance of the loop and its conjugate impedance (3 MHz to 12 MHz), calculated using Equations (8), (15), and a loop inductance value of 3.89 μH, are presented in Figure 7. These results were consistent with impedance calculations using *NEC*.

In order to ideally match ($\tau = 1$) the 1-m-diameter loop to a receiving system, the load impedance at its feed point had to be the conjugate of its feed-point impedance. From Figure 7, we saw that the impedance of the loop traversed the Smith chart clockwise, whereas its conjugate impedance traversed the Smith chart counterclockwise. It is well known that all passive impedances presented on the Smith chart must traverse it in the clockwise direction, thus indicating that implementation of a low-loss, broadband impedance match for the 1-m loop was not possible. This

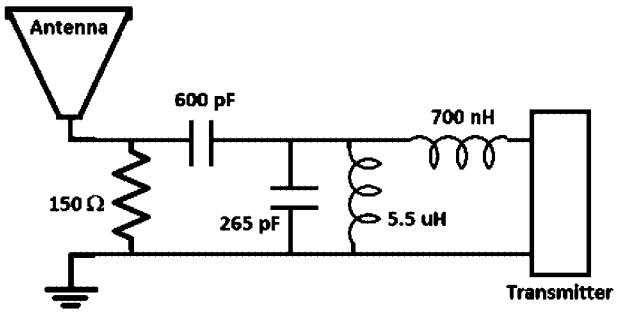

Figure 8. A depiction of the impedance network used to match the impedance of the 1 m diameter loop to a 50 ohm transmitter over the frequency range of 3 MHz to 12 MHz.

fact was consistent with the Chu limit for the quality factor of electrically small antennas and its relationship to matched-impedance bandwidth [17]. A broadband impedance match would require a lossy matching network.

To demonstrate several significant issues associated with impedance matching the receiving antenna, we started from the perspective of the transmitting antenna, where we required the *VSWR* looking from the transmitter into the matching network to be minimized. A lossy matching-network configuration that achieved a broadband match for the 1-m loop is presented in Figure 8. We assumed Q values of 800 and 60 for the capacitors and inductors, respectively. The corresponding input *VSWR* is presented in Figure 9. We saw that the 1-m loop was well matched with a *VSWR* less than 2:1 over the 3 MHz to 12 MHz frequency range.

To illustrate the differences between the matching-network characteristics when used in the transmitting mode versus the receiving mode, we first examined the network transfer function in the transmitting mode. The transfer

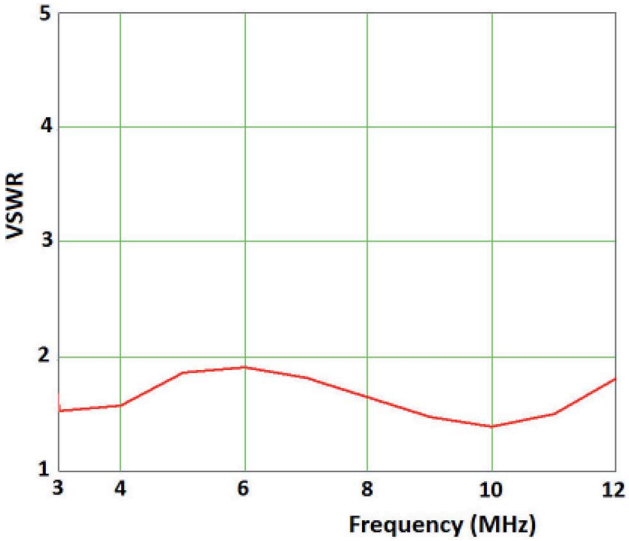

Figure 9. The *VSWR* at the input to the impedance matching depicted in Figure 8.

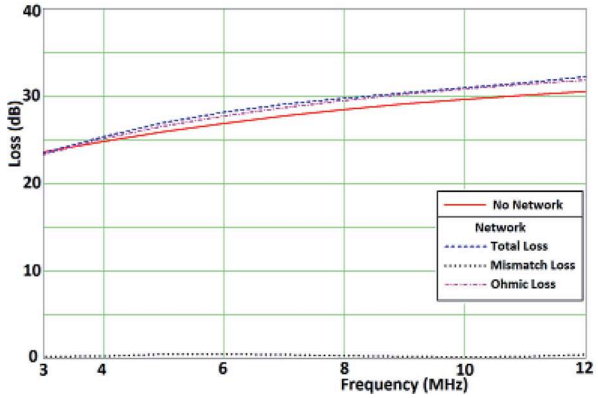

Figure 10. The transmitting mode network losses for the impedance-matching network depicted in Figure 8.

function – the network's total power loss between the transmitter and the antenna – is comprised of mismatch loss and ohmic losses. The network losses for the transmitting mode are presented in Figure 10. From Figure 10, we saw that the matching-network transfer function was dominated by the ohmic losses in the network components. Furthermore, while the antenna system was well matched to the transmitter, which delivered most of its power to the network input, the actual power delivered to the antenna was not substantially different than if the antenna was fed without the matching network. In fact, over most of the 3 MHz to 12 MHz frequency range, the total network loss was higher than the total loss with no network.

Next, we examined the matching network's transfer function in the receiving mode, where the antenna was delivering power to a 50-ohm receiver in place of the transmitter. The network losses for the receiving mode are presented in Figure 11. It was interesting to note that while the total network loss was the same as in the transmitting mode (maintaining reciprocity), the network losses were dominated by mismatch loss rather than ohmic losses. In this case, the network losses on receiving were minimal, and may have had little impact on the system's noise performance. In the receiving mode, the load impedance presented to the antenna was close to 50 ohms over the entire operating band, indicating that a receiving-mode matching

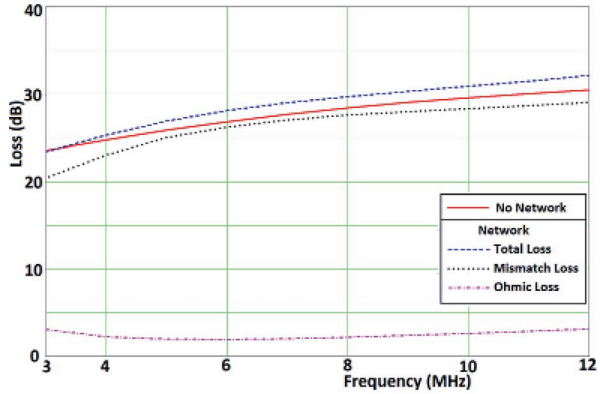

Figure 11. The receiving-mode network losses for the impedance-matching network depicted in Figure 8.

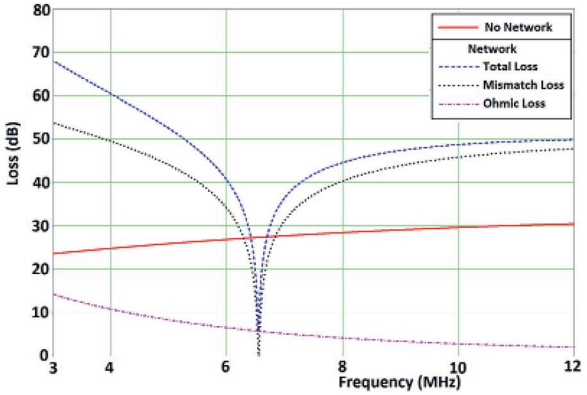

Figure 12. The receiving-mode network losses for an impedance-matching network designed to implement a conjugate match at 6.6 MHz.

network was of little value in the receiving system. In fact, the receive-mode transfer function (total loss) was higher than if the antenna was directly connected to the 50 ohm receiver. In many instances, particularly for broadband operation, receiving antennas do not necessarily require a matching network.

The next issue we considered is the implication of trying to optimize the receiving-mode impedance match at a single frequency by implementing a conjugate matched load at the antenna's feed point. For this exercise, a matching network was designed to implement a conjugate match at approximately 6.6 MHz. The corresponding network losses for the receiving mode are presented in Figure 12. While we were able to implement a near-perfect match and transfer function at 6.6 MHz, it came at the expense of very poor performance over the remainder of the frequency range. This was consistent with the fact that electrically small antennas have a very high quality factor, and cannot be impedance matched over a very wide operating bandwidth without significant loss.

In the design of the electrically small receiving antenna, it is extremely challenging to minimize the mismatch loss factor, τ, over a reasonable operating bandwidth. Oftentimes, the optimal solution is to simply forgo a matching network. Generally, the best design approach for the receiving system is to characterize the mismatch loss factor as a function of varying resistive load values, and to design to a load resistance that provides minimum mismatch loss over the desired operating band. This will oftentimes require an low-noise amplifier (low-noise amplifier) design or an impedance transformer to transform the 50 ohm receiver impedance to the desired load resistance value.

7. Ground Effects

The nature of HF systems is such that the HF antenna operates over the Earth ground plane, which has a significant impact on the antenna's overall efficiency and

radiation pattern. When operating over Earth ground, the overall efficiency of the antenna is diminished as a result of some portion of the delivered power being dissipated in the Earth. A portion of this ground-dissipated power propagates as a ground wave, sometimes over considerable distances. Here, we define the ground-loss efficiency, η_g, a factor that can be added to Equations (1) and (26) to account for the corresponding reduction in received power and the degradation of antenna sensitivity. Equations (1) and (26) become

$$P_r = P_d \tau \eta_r \eta_g \frac{\lambda^2 D}{4\pi} \tag{27}$$

and

$$S_P = \frac{4\pi k_b T_0}{\lambda^2 \tau \eta_r \eta_g D}, \tag{28}$$

respectively.

The determination of the ground-loss efficiency for the general antenna is not trivial. It varies as a function of frequency, ground properties (dielectric constant, ε_r, and conductivity, σ), antenna type (e.g., dipole versus loop), height above ground, and the antenna's orientation relative to the ground. Furthermore, the electrically small antenna's total feed-point resistance may not provide much if any insight into the level of ground loss, as it is often dominated by the copper loss resistance, and therefore does differ significantly over ground relative to the free-space value.

From an engineering design perspective, one of the most reliable methods for estimating ground loss is to use a Method-of-Moments simulation code, such as *NEC*. As examples of typical ground-loss values, we used *NEC* to simulate the efficiency of a dipole and circular loop over ground. Given the variables discussed above, a comprehensive study of ground loss is beyond the scope of this paper.

Here, we considered a 2 m (78.74 in) straight-wire dipole, having a conductor diameter of 5 mm (0.197 in), and a 1 m (39.37 in) diameter loop having a conductor diameter of 5 mm. The antennas were located at a height of 2 m, and were oriented both vertically and horizontally. The ground parameters were taken as average or medium soil with $\varepsilon_r = 13$ and $\sigma = 0.005$ S/m. The ground-effect efficiency for different configurations is presented in Figure 13.

From Figure 13, we saw that ground losses were more severe at low frequencies, and varied considerably as a function of the antenna's orientation relative to ground. Generally, the closer the antenna is to ground, the more severe the ground loss. In optimizing the placement of the electrically small receiving antenna, it is recommended that the antenna be located as high above ground as reasonably possible. Decisions regarding placement and orientation of the receiving antenna must consider the desired polarization and pattern shape, which dramatically vary relative to the well-known free-space patterns of the small loop and dipole. The ground parameters also have a significant effect on ground loss and, if possible, should be accurately estimated or determined to understand their impact on antenna performance.

Another point to note is that the ground-loss effect can be mitigated to some extent with an increase in the antenna's radiation resistance. However, that does not mean to imply that antennas with higher radiation resistance always have

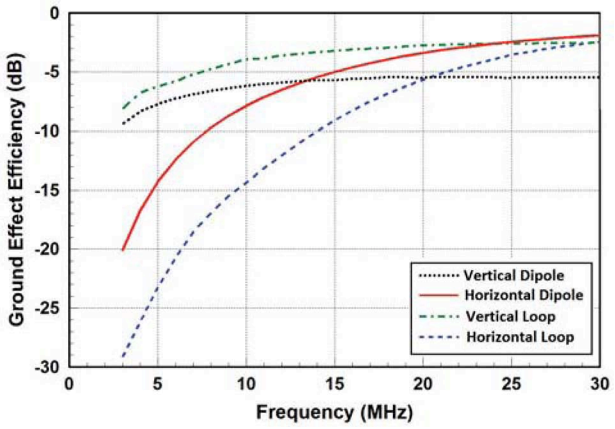

Figure 13. The ground loss efficiencies of the small dipole and loop as functions of frequency and orientation relative to ground.

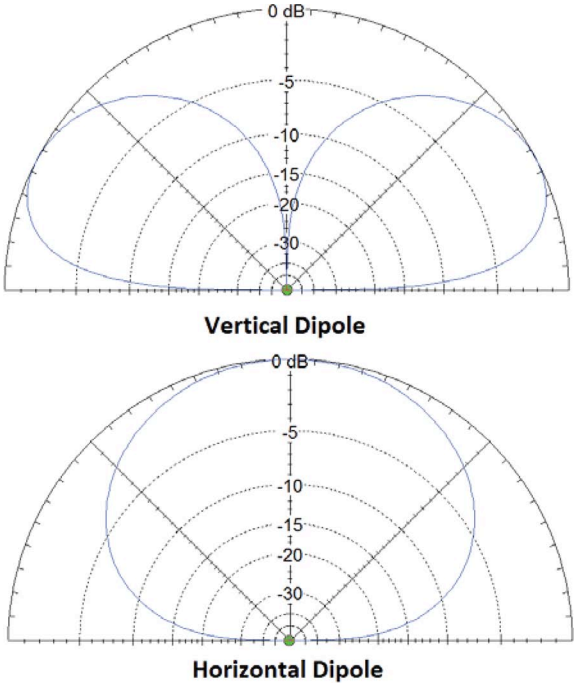

Figure 14. The radiation patterns of the vertical and horizontal 2 m dipole at 7.2 MHz. The antennas were at a height of 2 m above average soil.

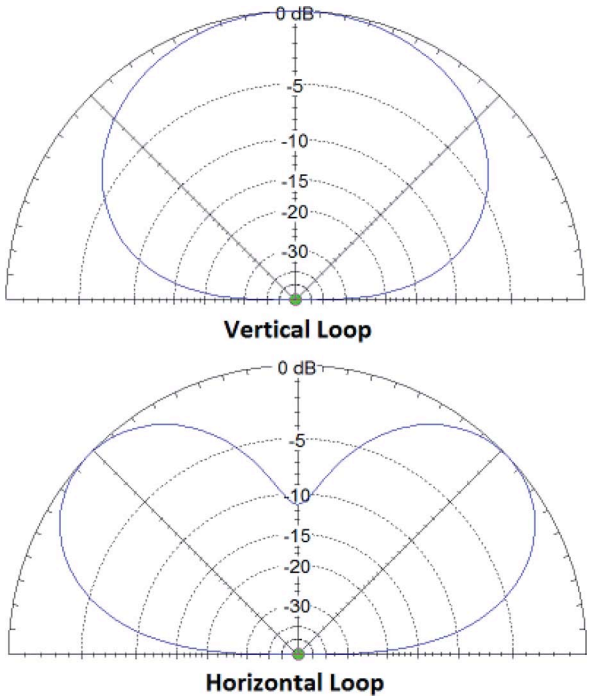

Figure 15. The radiation patterns of the vertical and horizontal 1 m diameter loops at 7.2 MHz. The antennas were at a height of 2 m above average soil.

better ground-loss performance. For example, the 2-m dipole had a much higher radiation resistance than the 1-m loop, but the vertical loop exhibited less ground loss than the vertical dipole. Generally, for the same antenna type (dipole-like or loop-like antennas), an increase in radiation resistance does offer ground-loss improvement. For example, a multi-turn loop with more turns will generally exhibit less ground loss than a similar sized loop with fewer turns.

The other significant effect of the ground is the impact on the small antenna's radiation pattern. To illustrate the significant effect of the ground on the antenna's radiation pattern, we again considered the 2-meter dipole and 1-meter diameter loop. Radiation patterns (elevation sweeps) for the vertical and horizontal dipole and loop are presented in Figures 14 and 15, respectively. The antennas were at heights of 2 m over average soil. The operating frequency was 7.2 MHz.

The radiation patterns of the simple elements over the lossy Earth ground were as expected. The horizontal dipole and vertical loop had the peak of their main beam directed overhead. Both were predominantly omnidirectional. Both responded to (receive) E-theta polarization in one elevation cut and to E-phi polarization in the orthogonal elevation cut. The inherent, bidirectional nulls of the vertical loop appeared at the lower elevations angles, but were not remarkable given that the lossy ground attenuated the far-field pattern at the lower angle. However, the elevation beamwidths were notably different in orthogonal elevation cuts.

The vertical dipole and horizontal loop exhibited omnidirectional radiation patterns with the expected nulls overhead. The vertical dipole responded to predominantly E-theta polarized signals, whereas the horizontal loop responded to predominantly E-phi polarized signals. We emphasize that both the dipole and loop responded to the EM wave, both its electric and magnetic fields. Notwithstanding near-field EM coupling, the idea that the dipole is uniquely an electric-field sensor and that the loop is uniquely a magnetic-field sensor is incorrect.

The radiation patterns at lower frequencies were much like those at 7.2 MHz. The patterns at higher frequencies changed as functions of the electrical size of the antenna and the differences in the electrical height above ground.

Determining the realized gain of the electrically small antenna requires knowledge of the antenna's mismatch loss, radiation efficiency, and ground loss. As expected, many electrically small antennas have very low gain, as will be discussed in subsequent sections.

8. External Noise, Noise Figure, and *SNR*

Prior to our discussion on external noise and signal-to-noise ratio in the HF receiving system, we emphasize that a detailed study of external noise properties, ionospheric propagation, and the propagation of the HF ordinary and extraordinary modes is beyond the scope of this paper. Here, we provide a general discussion on how the antenna's properties impact the *SNR* performance of the general receiving system, as well as methods for determining the system's noise figure and *SNR*.

In any receiving system, one must ensure that there is sufficient *SNR* at the detection point in the receiver in order to establish a successful link between the transmitter and the receiver. The required system *SNR* is a function of the system's waveform, modulation scheme, channel bandwidth, etc. Ultimately, the achieved *SNR* is limited by the noise floor of the receiver.

In low-frequency systems, such as HF, noise contributions to the receiving system are dominated by external background noise, which includes galactic noise, atmospheric noise, lightening, and man-made noise (e.g.,

Table 1. The coefficients for the calculation of the external noise figure.

Environment	*c*	*d*
Business	76.8	27.7
Interstate highway	73	27.7
Residential	72.5	27.7
Park and university campus	69.3	27.7
Rural	67.2	27.7
Quiet rural	53.6	28.6
Galactic noise	52	23

other radios, electrical equipment, motors, power supply noise, improper grounding, etc.). Ideally, we desire the HF system to be externally noise limited, that is, we do not want the internal noise contribution from the receiving system to be significant relative to the noise received or introduced by the antenna.

External noise is often difficult to predict, and varies significantly with the location of the receiving system and near-by manmade noise sources. External noise is generally not isotropic, nor is it necessarily predominant in one polarization. In the HF band, manmade noise often dominates the external noise levels. Noise predictions are often based on models of "typical" noise environments such as "*city*," "*residential*," "*rural*," and "*quiet-rural*," where the external noise figure, F_{am}, is given by [18, 19]

$$F_{am} = c - d\log(f), \tag{29}$$

where f is the frequency in MHz, and the coefficients c and d are given in Table 1. The external noise figure, F_{am} from Equation (29) is expressed in units of dB. We note that external noise-level predictions based on Equation (29) can put external noise levels at 20 dB to 60 dB higher than thermal noise ($k_b T_0$). The equivalent external "sky-temperature" based on the external noise figure is given by

$$T_E = (F_{am} - 1)T_0 \approx F_{am} T_0, \tag{30}$$

where F_{am} in Equation (30) is not expressed in dB. While the exact method for determining the external noise temperature seen by the antenna is to integrate the external noise sources over the antenna's directivity pattern, Equation (30) is generally taken as the external noise temperature in HF receiving systems. The external noise power seen by the antenna is then given by

$$N_e = k_b T_E B, \tag{31}$$

where B is the channel noise bandwidth in Hz. We note that the value of T_E is significantly higher than the Earth's ground temperature, and the noise contribution from the Earth's ground is therefore typically ignored.

In the design of HF receiving systems, the effects of the antenna's *VSWR* are often ignored, since the associated mismatch loss attenuates both external noise and the desired signal. However, if the external noise is sufficiently attenuated by the antenna's mismatch loss, it may approach the receiving system's noise floor and at some point, the receiving system will become internally noise limited. That said, we note that an internally noise-limited system does not preclude signal detection.

The receiving antenna will attenuate external signal and noise by the combined factors of mismatch loss, radiation efficiency, and ground loss. Furthermore, the antenna will introduce its own thermal-noise contribution, which is only attenuated by the antenna's mismatch loss. The total noise contribution to the receiving system from the antenna is given by [20]

$$N_{et} = k_b\left[\tau\eta_r\eta_g T_E + \tau(1-\eta_r)T_p\right]B, \tag{32}$$

where T_p is the physical temperature of the antenna, often assumed to be equal to T_0. The equivalent noise temperature for the antenna is simply given by

$$T_A = \tau\eta_r\eta_g T_E + \tau(1-\eta_r)T_p. \tag{33}$$

To ensure that the receiving system is externally noise limited, the antenna's noise temperature must be greater than the receiving system's noise temperature, T_R as defined at the antenna's feed point. From an antenna performance-optimization perspective, it is obvious that the design objectives are to minimize mismatch loss, maximize radiation efficiency, and minimize ground loss. This is entirely consistent with the antenna's receiving sensitivity as defined in Equation (28).

To better quantify and compare the antenna's receiving performance, we consider a simple receiving system as depicted in Figure 16. Figure 16 illustrates a receiving system where a balanced antenna (dipole or loop) requires a balun; a bandpass filter (BPF) is placed before the low-noise amplifier (LNA); and a coaxial cable is used to connect the low-noise amplifier to the receiver. The bandpass filter is placed before the low-noise amplifier so as to preclude external signals outside of the HF band from entering the low-noise amplifier and being amplified. This helps mitigate low-noise-amplifier saturation, and prevents possibly high levels of out-of-band noise from entering the receiver. We place the low-noise amplifier as close to the antenna's feed point as possible to optimize *SNR* performance.

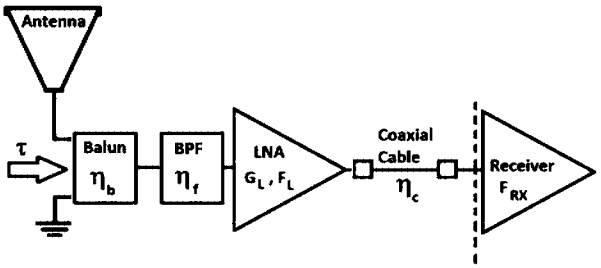

Figure 16. A depiction of a simple HF receiving system comprised of a balun, bandpass filter, low-noise amplifier, and coaxial cable.

The terms η_b, η_f, and η_c are the efficiencies of the balun, bandpass filter, and coaxial cable, respectively. The terms G_L and F_L are the gain and noise figure of the low-noise amplifier, and F_{RX} is the receiver's noise figure. In optimizing the receiving antenna, there are a number of ways to characterize its performance. We typically characterize the receiving antenna's noise figure relative to a lossless, matched antenna; however, this may not provide direct insight into whether-or-not the actual receiving system will meet the *SNR* requirements. Unfortunately, determination of the system *SNR* requires a detailed link analysis with knowledge of the incident signal power density and external noise levels.

Calculation of the antenna's noise figure relative to the lossless matched antenna can be done assuming both are connected to a receiving system having a noise temperature, T_R, defined at the antenna's feed point. To determine the actual performance of the receiving system, we need to ultimately determine the actual *SNR* at the detection point in the receiver as a function of the received signal, external noise, the antenna's performance properties, and the receiving system's noise figure, T_R.

Given the calculated external noise power in Equation (31), it is necessary to define the corresponding external signal power available to the general receiving antenna, S_i. This is given by the maximum power the general antenna is capable of receiving:

$$S_i = P_d \frac{\lambda^2 D}{4\pi}. \tag{34}$$

The general receiving antenna's noise figure can be found from SNR_i/SNR_0, where SNR_i is the ratio S_i/N_e and SNR_0 is the actual *SNR* established in the receiving system. The *SNR* established in the system, SNR_0, is given by [20]

$$SNR_0 = \frac{\tau\eta_r\eta_g S_i}{k_b\left[\tau\eta_r\eta_g T_E + \tau\left(1-\eta_r\right)T_p + T_R\right]B} \tag{35}$$

$$= \frac{\tau\eta_r\eta_g S_i}{k_b\left(T_A + T_R\right)B}.$$

The numerator of Equation (35) is the received power delivered to the receiving system at the antenna's feed point, and the denominator is the total noise in the receiving system including the attenuated external noise, the noise contribution from the antenna's ohmic losses, and the internal noise contribution from the receiving system, where all are defined at the antenna's feed point. The noise figure of the general receiving antenna relative to that of a lossless matched antenna connected to the same receiving system, F_{ar}, is then given by [20]

$$F_{ar} = \frac{T_A + T_R}{\tau\eta_r\eta_g\left(T_E + T_R\right)}. \tag{36}$$

Equation (36) can be used to characterize the noise-figure performance of any receiving antenna relative to an ideal, lossless, matched antenna. Equation (35) can be used to determine the actual *SNR* in the receiving system. The receiving system's noise temperature, T_R, is found by cascading all of the system's internal noise contributions and referencing them to the antenna's feed point. For the simple receiving system shown in Figure 16, T_R is given by

$$T_R = \frac{\left(F_{RX}-1\right)T_0}{\eta_c G_L\eta_f\eta_b} + \frac{\left(1-\eta_c\right)T_p}{\eta_c G_L\eta_f\eta_b} + \frac{\left(F_L-1\right)T_0}{\eta_f\eta_b}$$

$$+ \frac{\left(1-\eta_f\right)T_p}{\eta_f\eta_b} + \frac{\left(1-\eta_b\right)T_p}{\eta_b}. \tag{37}$$

In cascading the internal noise to the antenna feed point, we assumed that all of the components were matched at the input and output. Any high *VSWRs* would have to be taken into consideration in the noise temperature and *SNR* analysis of a real system. Finally, we note that the receiving sensitivity expressions developed in the previous sections are not valid for comparing the relative performance of the electrically small antenna in terms of realized system *SNR*.

9. Optimization Examples: The Dipole, Circular Loop, and the Multi-Turn Loop

In this section, we consider the optimization of the performance properties of the general, electrically small HF receiving antenna. Specifically, we consider the straight-wire dipole, the circular loop, and the multi-turn loop. The relative performance of the different antenna designs is based on the antenna's noise figure relative to the lossless, matched antenna as defined in Equation (36).

Optimization of the electrically small receiving antenna is primarily a function of its radiation efficiency and the impedance match to the receiving system, the first component of which is often a low-noise amplifier. Oftentimes, the impedance match to the low-noise amplifier

is critical in optimizing *SNR* performance, particularly over wide-bandwidth operation.

Electrically small dipoles have high radiation efficiency, provided they are constructed using reasonable conductor diameters. For example, at 3 MHz, the radiation efficiency of a 50 cm (19.685 in) dipole, constructed using 10 AWG copper wire ($d = 2.588$ mm $= 0.1019$ in), is approximately 35%. A 2 m (78.74 in) dipole has a radiation efficiency of approximately 68%. The challenge with the electrically small dipole is that that its capacitive reactance is very high, making it difficult to impedance match, particularly to low impedance values such as 50 ohms. This can be an issue if one intends to use a 50-ohm low-noise amplifier in the receiving system.

The loop antenna differs significantly from the dipole in that it has a substantially lower radiation efficiency for the same conductor length. For example, a 50 cm (19.685 in) circumference circular loop (~ 16 cm or 6.3 in diameter), constructed with 10-guage copper wire, has a radiation efficiency of approximately 4×10^{-4}%. The 1 m (39.37 in) diameter loop ($C \approx 3.14$ m ≈ 123.6 in) has a radiation efficiency of approximately 11%. The advantage of the single-turn loop antenna is that it has a relatively low inductance reactance, which may provide a better match to a 50 ohm low-noise amplifier. The other advantage of the loop is that multiple turns and a ferrite core can be added to substantially increase its radiation efficiency. However, ferrite-core loops generally have small diameters (small areas), making dipole-like radiation efficiencies difficult to achieve. The other issue to consider with the multi-turn air- and ferrite-core loop is that their impedances tend to approach anti-resonance at higher frequencies, which may make optimization of the impedance match to a low-noise amplifier difficult, particularly over wide impedance bandwidths. We note that the small loop can be used as a receiving antenna near anti-resonance and its performance, like all antennas, is a function of mismatch loss, radiation efficiency, and ground loss.

In selecting the antenna design and orientation of the HF receiving antenna, one may also consider the propagation mode (ground wave, near-vertical-incidence, NVIS, single-hop, or multiple-hop) and the associated frequency range. These topics are beyond the scope of this paper and the examples presented in this section. Here, we consider the vertical and horizontal dipole and loop, and compare their performance properties over the HF band.

With any electrically small antenna, its overall performance properties are optimized by making the antenna as large as reasonably possible. This aids in optimizing both the impedance match and the radiation efficiency. Here, we considered a 2 m (78.74 in) dipole, a 1 m (39.37 in) circular loop, and a multi-turn loop, with the objective of optimizing their noise-figure performance. The antennas were assumed to be at a height of 2 m over average soil. Given a fixed antenna size, the radiation efficiency was

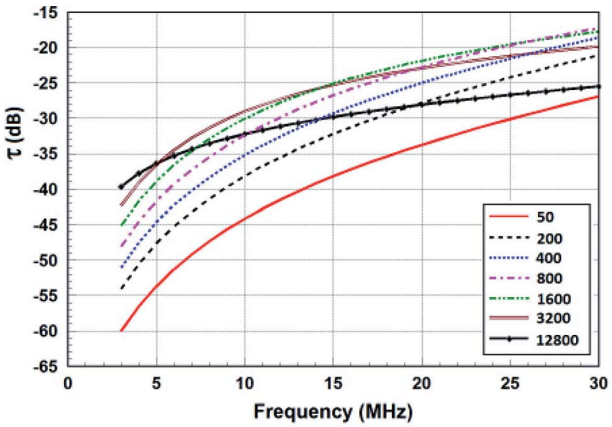

Figure 17. The values of τ in dB for the 2 m dipole as a function of load resistance.

optimized by using as large a conductor diameter as was reasonably possible. Here, we chose to use 10 AWG copper wire. The mismatch loss was optimized by implementing a receiving-system impedance that minimized the calculated value of τ over the HF operating band. Generally, the best optimization process is to calculate τ for a variety of real load impedances ($X_L = 0$), and to implement the load resistance that provides the minimum average τ over the operating band. Implementing arbitrary values of load resistance may be difficult, given the necessity of working with 50 ohm systems. One approach is to use an impedance transformer and/or low-noise amplifier that transforms the system's 50 ohm impedance to close to the desired load resistance. Impedance transformers are typically available, or can be designed in a wide range of transformation ratios (e.g., 2:1, 3:1, 4:1, 8:1, 16:1, 32:1, etc.). Finally, we caution against attempting to tune and match the antenna at a single frequency, as this often significantly degrades performance at other frequencies.

For the 2 m dipole, we used *NEC* simulations to calculate τ as a function of varying load resistance, with the results presented in Figure 17. The optimum value of load resistance was between 1600 ohms and 3200 ohms. At

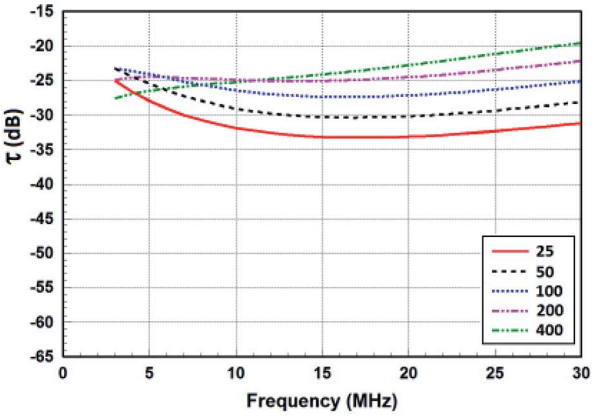

Figure 18. The values of τ in dB for the 1 m loop as a function of load resistance.

values of load resistance above 12800 ohms, the mismatch loss began to worsen over the entire band. A load resistance of 1600 ohms (32:1 transformer) improved the mismatch loss by approximately 15 dB at 3 MHz, and 10 dB at 30 MHz.

We next considered the 1 m loop, and again used *NEC* to calculate the value of τ as a function of load resistance, with the results presented in Figure 18. The optimum value of load resistance was approximately 200 ohms. At higher values of load resistance, the mismatch loss began to degrade at the lower frequencies. While the 1 m loop was less efficient than the 2 m dipole, we noted that its mismatch loss was substantially better over most of the HF band. We noted that the results in Figures 17 and 18 held for both the vertical and horizontal orientations, as the impedance did not significantly change with the change in orientation.

Using *NEC*, we simulated the value of radiation efficiency and ground loss for the dipole and loop, and calculated their noise figures. We assumed a receiving system (Figure 16) with a balun transformer having 0.25 dB loss; a bandpass filter with 0.25 dB loss; a low-noise amplifier with a gain of 30 dB and a noise figure of 1.5 dB; a coaxial cable with 2 dB loss; and a receiver with a 5 dB noise figure. The resulting value of T_R was 170.924K. The dipole and loop noise figures are presented in Figure 19. We calculated the external background noise using Equation (29), assuming "*galactic*" noise levels. We assumed a load resistance of 1600 ohms for the dipole and 200 ohms for the loop. From Figure 19, we saw that the dipole antenna had better noise-figure performance than the loop, and that the vertical orientations exhibited better noise figures than the horizontal orientations. We also noted that the noise figure improved with increasing levels of external noise. The external "*galactic*" noise level chosen here predicted the most conservative or pessimistic antenna performance.

In and of itself, the noise figure of the antenna does not provide a precise indication as to whether or not the HF receiving system is internally or externally noise limited. The

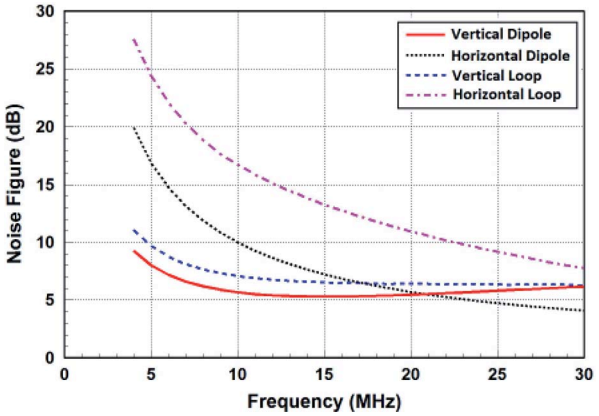

Figure 19. The noise figures of the 2 m dipole and 1 m loop located 2 m over average soil. The external noise level was assumed to be "*galactic*."

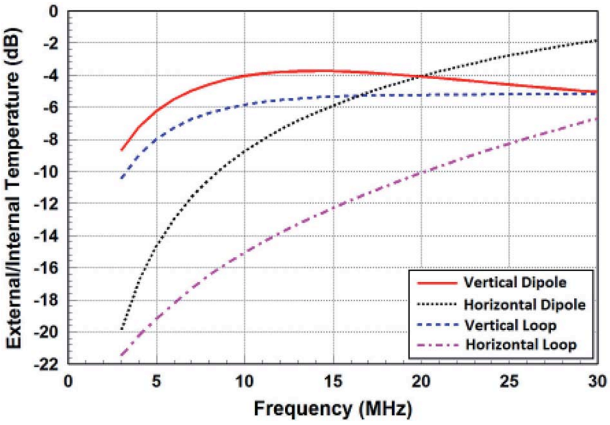

Figure 20. The ratio of external background noise temperature to the receiving system's internal noise temperature for the 2 m dipole and 1 m loop located 2 m over average soil. The external noise level was assumed to be "*galactic*."

system will be externally noise limited when the antenna's noise temperature, T_A, is greater than the receiving system's noise temperature, T_R. The ratios of T_A/T_R for the 2 m (78.74 in) dipole and the 1 m (39.37 in) loop are presented in Figure 20. From Figure 20, we saw that these antenna designs were not externally noise limited: rather, they were internally noise limited. We emphasize that the assumed external background noise level was "*galactic*," and note that with an increase in external background noise level, the receiving system tends to become externally noise limited. However, determining whether a link can be established between the transmitting and receiving system requires a link-budget analysis to determine the actual *SNR* in the receiver.

The next example was the optimization of an electrically small multi-turn loop. The design objective with the small multi-turn loop was to minimize the overall size of the receiving antenna, and to achieve reasonable values of radiation efficiency and mismatch loss. Here, we used the 1 m (39.37 in) loop as a reference design.

Considering the 1 m loop in free space, the radiation efficiency at 3 MHz was calculated to be –29.66 dB using *NEC* and –29.57 dB using theory. We choose a small loop diameter of 7.63 cm (3.00 in) so as to make the use of a ferrite core reasonable. With this loop diameter, over 2000 turns were required when using an air core to achieve the same efficiency as the 1 m loop. When using a ferrite core with $\mu_{fr} = 100$ and a cylindrical length of 20 cm (7.84 in), approximately 25 turns were required to achieve the same

Table 2. The radiation-efficiency calculations for the 22-turn loop at 3 MHz (values are in dB).

Loop Configuration	Theory	*NEC*	*FEKO*
Air-Core	–49.24	–49.15	–49.31
Ferrite-Core	–29.62	N/A	–29.9

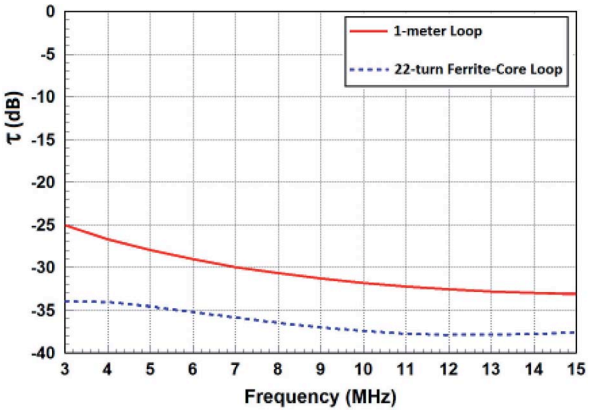

Figure 21. The values of τ for the 1 m air-core loop and the 22-turn ferrite-core loop.

efficiency as the 1 m loop. To validate these estimates and the noise-figure calculations that followed, we compared theory and simulation using *NEC* and *FEKO* [21] to model 22-turn air-core and ferrite-core loops. We determine their radiation efficiencies at 3 MHz. The numerical results are presented in Table 2.

Using the impedance-matching optimization procedure previously discussed, we found that a load impedance of 3200 ohms provided an optimum value of mismatch loss for the ferrite-core loop. We noted that the 22-turn ferrite-core loop exhibited an anti-resonance at approximately 9 MHz, which had minimal impact on the optimized mismatch loss. The mismatch loss and noise figure of the 22-turn ferrite-core loop over a frequency range of 3 MHz to 15 MHz is compared to that of the 1 m air-core loop in Figures 21 and 22, respectively.

We saw from Figure 21 that the mismatch loss between the two antenna designs varied from approximately 10 dB at 3 MHz to 5 dB at 15 MHz. This difference in mismatch loss accordingly impacted the difference in noise figure. In addition to the differences in mismatch loss, the noise figures also differed due to differences in their ohmic and ground losses as a function of frequency. We saw that the

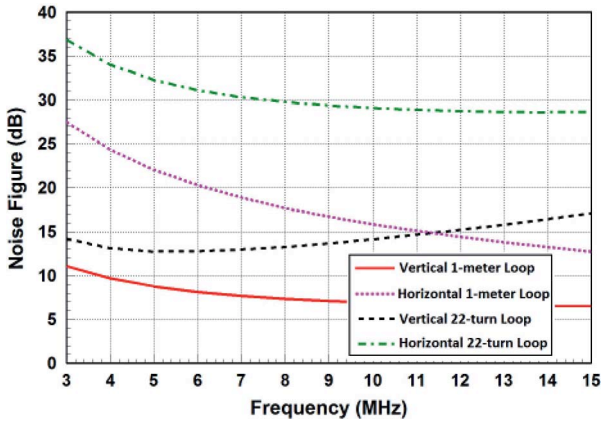

Figure 22. A comparison of the noise figures of the 1 m air-core loop and the 22 turn ferrite-core loop.

small ferrite-core loop, designed to match the free-space efficiency of the 1 m loop, did not perform as well as the 1 m loop operating over Earth ground.

10. Summary

In the design of electrically small antennas, there is always some amount of performance tradeoff in terms of mismatch loss and radiation efficiency. Ultimately, optimizing the design of the electrically small receiving antenna is a function of maximizing the antenna size as much as is reasonably possible, optimizing the load impedance seen by the antenna, improving the radiation efficiency as much as possible, and minimizing the internal losses in the receiving system. To fully characterize the absolute or relative performance of the receiving antenna, one can use the formulas for receiving sensitivity, noise figure, and compare the ratio of antenna noise temperature to the receiving system's noise temperature.

11. References

1. R. J. Eassom, R. L. J. Awcock, and B. M. Sosin, "HF Transmitters and Receivers for Naval Radio," IEE 1995 International Conference on 100 Years of Radio, London, UK, September 1995, pp. 62-68.

2. J. Maxwell, "Amateur Radio: 100 Years of Discovery," *ARRL QST*, January 2000.

3. D. H. Sinnott, "The Development of Over-The-Horizon Radar in Australia," DSTO, 1988.

4. R. C. Daniels and S. W. Peters, "A New MIMO HF Data Link: Designing for High Data Rates and Backwards Compatibility," IEEE MILCOM Conference, San Diego, CA, November 2013, pp. 1256-1261.

5. M. P. Scheible, L. J. Teig, J. D. Fite, K. M. Cuomo, J. L. Werth, G. W. Meurer, N. C. Ferreira, and C. R. Franzini, "High Data Rate, Reliable Wideband HF Communications Demonstration," MITRE Technical Paper, www.mitre.org, 2014.

6. U. S. Navy, "Electronics Technician, Vol. 7 – Antennas and Wave Propagation," NAVEDTRA 14092, October 1995, Chapter 2, pp. 2-7 – 2-14.

7. J. S. Belrose, "Radiation Characteristics of an Electrically Small MF Antenna – By Simulation," IEE International Conference on Antennas and Propagation, April 2001, pp. 90-94.

8. G. Lasser, M. Ignatenko, and D. Filipovic, "Tuning an Electrically Small On-the-Move HF Half-Loop Antenna," 10th European Conference on Antennas and Propagation (EuCAP), April 2016.

9. J. Baker and M. F. Iskander, "New Design Methodology for Electrically Small HF Antenna," IEEE International Symposium on Antennas and Propagation, Memphis, TN, July 2014.

10. C. A. Balanis, *Antenna Theory: Analysis and Design*, New York, John Wiley & Sons, 2005.

11. S. R. Best and B. C. Kaanta, "A Tutorial on Receiving and Scattering Properties of Antennas," *IEEE Antennas and Propagation Magazine*, **51**, 5, October 2009, pp. 26-37.

12. S. R. Best, "On the Performance Properties of the Koch Fractal and Other Bent Wire Monopoles," *IEEE Transactions on Antennas and Propagation*, **51**, 6, June 2003, pp. 1292-1300.

13. S. R. Best and A. D. Yaghjian, "The Lower Bounds on *Q* for Lossy Electric and Magnetic Dipole Antennas," *IEEE Antennas and Wireless Propagation Letters*, **3**, 2004, pp. 314-316.

14. A. Yaghjian, *private communication.*

15. S. K. Harriman, E. W. Paschal, and U. S Inan, "Magnetic Sensor Design for Femtotesla Low-Frequency Signals," *IEEE Transactions on Geoscience and Remote Sensing*, **48**, 1, January 2010, pp. 396-402.

16. Gerald J. Burke, "The Numerical Electromagnetics Code – NEC 4, Method of Moments," Lawrence Livermore National Laboratory, January 1992.

17. A. D. Yaghjian and S. R. Best, "Impedance, Bandwidth and *Q* of Antennas," *IEEE Transactions on Antennas and Propagation*, **53**, 4, April 2005, pp. 1298-1324.

18. Radio Noise, Recommendation ITU-R P.370-10 (10/2009), ITU-R.

19. S. W. Ellignson, "Antennas for the Next Generation of Low-Frequency Radio Telescopes," *IEEE Transactions on Antennas and Propagation*, **54**, 8, August 2005, pp. 2480-2489

20. S. R. Best, "Realized Noise Figure of the General Receiving Antenna," *IEEE Antennas and Wireless Propagation Letters*, **12**, 2013, pp. 702-705.

21. FEKO, https://www.feko.info/.

Introducing the Author

Steven R. Best is a Senior Principal Sensor Systems Engineer with the MITRE Corporation in Bedford, MA, USA. He received the BScEng and the PhD in Electrical Engineering in 1983 and 1988 from the University of New Brunswick in Canada. He has over 28 years of experience in business management and antenna design engineering in both military and commercial markets. Prior to joining MITRE, he was with the Air Force Research Laboratory (AFRL) at Hanscom AFB. Prior to joining AFRL, he was with Cushcraft Corporation in Manchester, NH, from 1997 to 2002. He was Director of Engineering at Cushcraft from 1996 to 1997. Prior to joining Cushcraft, he was with Parisi Antenna Systems from 1993 through 1996. He was with D&M/Chu Technology, Inc. (formerly Chu Associates) from 1990-1993. He joined Chu Associates as a Senior Electrical Engineer in 1987.

Dr. Best is the author or coauthor of three book chapters and over 100 papers in various journal, conference, and industry publications. He frequently presents a three-day short course for the wireless industry titled "Antennas and Propagation for Wireless Communication," and he has presented several webinars on antenna topics. He has also authored an IEEE Expert Now module on electrically small antennas. He is a former Distinguished Lecturer for AP-S, a former member of the AP-S AdCom, a former Associate Editor for the *IEEE Transactions on Antennas and Propagation*, and Senior Past Chair of the IEEE Boston Section. He is a former AP-S Electronic Communications Editor-in-Chief. Dr Best is a Fellow of the IEEE and a former President of AP-S.